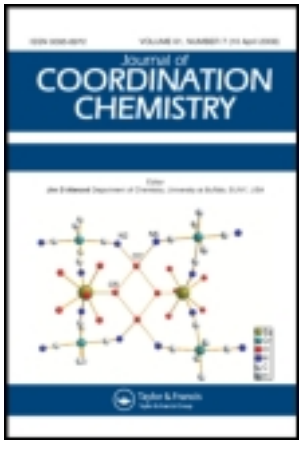

Journal of Coordination Chemistry
Publication details, including instructions for authors and subscription information:
http://www.tandfonline.com/loi/gcoo20

Dinuclear copper(II) complexes of Fenoprofen: synthesis, spectroscopic, thermal, and SOD-mimic activity studies

M.A. Agotegaray [a], M.A. Boeris [b], A.S. Diez [a], M.R. Prat [a] & O.V. Quinzani [a]

[a] Departamento de Química, INQUISUR, Universidad Nacional del Sur, Avda. Alem 1253, B8000CPB Bahía Blanca, Argentina

[b] Facultad de Ciencias Veterinarias, Centro de Investigación y Desarrollo de Fármacos (CIDEF), Universidad Nacional de La Pampa, Calle 5y 116, General Pico, CP 6360, Argentina

Published online: 07 Jul 2011.

To cite this article: M.A. Agotegaray, M.A. Boeris, A.S. Diez, M.R. Prat & O.V. Quinzani (2011) Dinuclear copper(II) complexes of Fenoprofen: synthesis, spectroscopic, thermal, and SOD-mimic activity studies, Journal of Coordination Chemistry, 64:13, 2246-2261, DOI: 10.1080/00958972.2011.594508

To link to this article: http://dx.doi.org/10.1080/00958972.2011.594508

Journal of Coordination Chemistry
Vol. 64, No. 13, 10 July 2011, 2246–2261

Dinuclear copper(II) complexes of Fenoprofen: synthesis, spectroscopic, thermal, and SOD-mimic activity studies

M.A. AGOTEGARAY*†, M.A. BOERIS‡, A.S. DIEZ†, M.R. PRAT† and O.V. QUINZANI†

†Departamento de Química, INQUISUR, Universidad Nacional del Sur, Avda. Alem 1253, B8000CPB Bahía Blanca, Argentina
‡Facultad de Ciencias Veterinarias, Centro de Investigación y Desarrollo de Fármacos (CIDEF), Universidad Nacional de La Pampa, Calle 5y 116, General Pico, CP 6360, Argentina

(*Received 8 February 2011; in final form 4 May 2011*)

Three dinuclear copper(II) complexes with the anti-inflammatory drug Fenoprofen [Hfen, 2-(3-phenoxyphenyl)propionic acid] and nitrogen donors of general formula $[Cu_2(fen)_4(L)]_n$ were prepared from $[Cu_2(fen)_4(dmf)_2]\cdot 2H_2O$ (**1**) [dmf = *N*,*N*′-dimethylformamide; L = 4,4′-bipyridine (**2**), pyrazine (**3**), and 2,5-dimethylpyrazine (**4**)]. The new complexes were characterized by chemical analysis, spectroscopic, and thermogravimetric techniques. Antioxidant properties of **1–4** were evaluated for superoxide-dismutase-mimic activity employing the XTT method. Complex **2** presented the highest antioxidant activity ($IC_{50} = 0.260\ \mu mol\ L^{-1}$). Anti-inflammatory properties of **2** were evaluated employing carrageenan-induced paw edema in mice, revealing that the Fenoprofen–copper(II) complex containing 4,4′-bipyridine does not present enhanced anti-inflammatory activity compared to the uncomplexed parent drug Fenoprofen calcium salt.

Keywords: Copper; Fenoprofen; Spectroscopy; SOD; Anti-inflammatory

1. Introduction

The synthesis, structural characterization, and evaluation of pharmacological activity of metal complexes of non-steroidal anti-inflammatory drugs (NSAIDs) as ligands has acquired increased importance because of improved properties of the metal complexes when compared to free ligands [1]. The metal–NSAID association seems to play a specific role taking into account the hypothesis advanced by Sorenson and co-workers [2–5] that copper complexes are the active form of these drugs. Copper is the third most abundant transition metal element in biological systems [6] and plays an important role in a series of biological functions, electron transport, oxidase systems, transport of oxygen, and dismutation of the superoxide radical [superoxide dismutase (SOD)] [7]. It is believed to possess anti-inflammatory activity itself [5–8] because an increased demand for copper during inflammatory conditions [9] has been proven.

*Corresponding author. Email: magotegaray@uns.edu.ar

ISSN 0095-8972 print/ISSN 1029-0389 online © 2011 Taylor & Francis
DOI: 10.1080/00958972.2011.594508

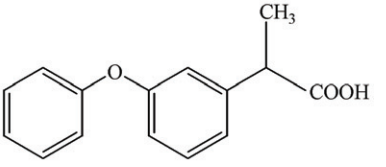

Scheme 1. Molecular structure of Fenoprofen.

Fenoprofen, 2-(3-phenoxyphenyl)propionic acid or *a*-methyl-3-phenoxybenzeneacetic acid (scheme 1) is a non-steroidal anti-inflammatory, antipyretic, and analgesic drug [10, 11], belonging to the group of compounds commonly referred to as 2-arylpropionic acids. It has a chiral carbon resulting in two possible enantiomers, R(−) and S(+). Recently, the resolved R and S isomers and the R–S racemate of Fenoprofen were compared *in vitro* as inhibitors of the fatty acid cyclooxygenase system from human platelets, indicating that the anti-inflammatory activity could be associated with the inhibition of prostaglandin synthesis [12].

We recently proved that the dinuclear copper complex $Cu_2(fen)_4(dmf)_2$ (fen = fenoprofenate anion) presents enhanced anti-inflammatory activity over the marketed form of the parent drug Fenoprofen calcium dihydrate [13]. Some copper–NSAID complexes do not present enhanced anti-inflammatory activity when compared to the uncomplexed parent drug. This is the case for Flurbiprofen copper(II) complex which has similar *in-vivo* anti-inflammatory activity to free Flurbiprofen [14].

Reactivity studies of bimetallic copper(II) complexes as model compounds for metalloenzymes is of interest for the development of bio-inspired catalysts [15]. Many copper(II) complexes with NSAIDs have SOD activity. The Cu–Zn SOD (Cu–ZnSOD) is a metalloprotein discovered by Fridovich and McCord in 1969 [16] and represents the defense system against the cytotoxicity caused by superoxide radicals (O_2^-). They belong to the family of reactive oxygen species known as ROS and induce cell and molecular damage when reacting with biomolecules, such as deoxyribonucleic acid (DNA), lipids, and proteins, under oxidative stress conditions [17]. The catalytic role of Cu–ZnSOD is based on the reaction between two molecules of superoxide to produce hydrogen peroxide and molecular oxygen by a cyclic Cu(II)–Cu(I) redox reaction [1]. The use of SOD as a pharmaceutical has been proposed for the treatment of a number of diseases including inflammation and inflammation-associated diseases [18], because the removal of potentially damaging superoxide radical (O_2^-) would protect against the development of inflammation.

Interested in the effects of axial ligands on properties of the dinuclear cage "$Cu_2(fen)_4$", we prepared new derivatives with mono and bidentate ligands. Bidentate diazines are good coordinating agents for copper(II) [19] and have been extensively used for the design of oligomeric and polymeric complexes as part of the chemistry of 1-D, 2-D, and 3-D metal carboxylates [20, 21]. A polymeric complex of 4,4′-bipyridine and copper valproate, $[Cu_2(val)_4(4,4'\text{-bipy})]_n$, showed SOD-mimic properties [22]; as far as we know, no other polymeric Cu(II)–NSAID complex has been studied until now.

In this article we present the synthesis, spectroscopic characterization, and thermal behavior of three new polymeric fenoprofenate copper(II) complexes containing three diazines that can act as exo-bidentate ligands: 4,4′-bipyridine, pyrazine, and 2,5-dimethylpyrazine. We also present their SOD-mimic activity as well as the *in vivo* study

of anti-inflammatory properties of one of the new compounds employing the carrageenan-induced paw edema in mice.

2. Experimental

2.1. *Materials and general procedures*

All reagents were of commercial analytical quality and have been used without purification. $[Cu_2(fen)_4(dmf)_2]\cdot 2H_2O$ (**1**) was prepared following the procedure published elsewhere [13]. Carbon, hydrogen, and nitrogen analyses have been performed using a Carlo Erba EA 1108 instrument. Copper was determined employing a GBC 932 Atomic Absorption Spectrophotometer after an acid digestion of the samples with a volume ratio $HCl : HNO_3 = 1 : 1$.

2.2. *Synthesis of the complexes*

2.2.1. $[Cu_2(fen)_4(4,4'\text{-bipy})]_n$ (2). Compound **2** was prepared from mixing 2.00 mL of an acetone solution containing 64.0 mg (5.00×10^{-2} mmol) of **1** with 7.8 mg (5.0×10^{-2} mmol) of 4,4′-bipyridine dissolved in 1.0 mL of acetone. The resulting solution was stirred for 1 h at laboratory temperature. After the addition of 2.50 mL of acetonitrile, the homogeneous mixture was kept at 4°C until a precipitate was obtained. The green solid was filtered, washed with acetonitrile, and air dried. Analysis calculated for $C_{70}H_{60}Cu_2N_2O_{12}$ (%): C, 67.37; H, 4.81; N, 2.24; Cu, 10.18. Found (%): C, 67.30; H, 4.70; N, 2.10; Cu, 9.74. Yield: 80.4%.

2.2.2. $[Cu_2(fen)_4(pyz)]_n$ (3). The pyrazine derivative was prepared following the procedure employed for **2**, using 4.0 mg (5.0×10^{-2} mmol) of pyrazine. Analysis calculated for $C_{64}H_{56}Cu_2N_2O_{12}$ (%): C, 65.57; H, 4.78; N, 2.39; Cu, 10.85. Found (%): C, 65.50; H, 4.10; N, 2.30; Cu, 10.40. Yield: 79.2%.

2.2.3. $[Cu_2(fen)_4(2,5\text{-}Me_2pyz)]_n$ (4). The 2,5-dimethylpyrazine derivative was prepared following the procedure employed for **2**, using 5.4 mg (5.0×10^{-2} mmol) of the diazine. Analysis calculated for $C_{66}H_{60}Cu_2N_2O_{12}$ (%): C, 66.05; H, 5.00; N, 2.33; Cu, 10.60. Found (%): C, 65.93; H, 5.06; N, 2.60; Cu, 10.60. Yield: 74.5%.

2.3. *Spectroscopic and thermal analysis of the substances*

EPR spectra of solid samples were obtained at room temperature with a Bruker ER200 spectrometer, operating at X band (~9.8 GHz), with a Bruker cavity and a modulation field of 100 KHz. IR spectra were recorded in KBr pellets with a Nicolet Nexus FT-IR spectrophotometer from 400 to 4000 cm^{-1} and UV-Vis spectra were registered on GBC-Cintra 20 equipment from 190 and 900 nm.

Thermogravimetric analyses (TGA) and differential thermal analyses (DTA) were carried out on a Rigaku Thermoflex TG 8110, coupled to a Thermal Analysis Station

TAS 100 thermal analyzer apparatus, under a nitrogen flow of $20\,cm^3\,min^{-1}$ up to a final temperature of 850°C. The heating rate was $5°C\,min^{-1}$ and sample masses were about 6.0 mg. Al_2O_3 was used as a DTA reference standard. For differential scanning calorimetry (DSC) analysis a TA Instrument Q20 was employed, using In as a reference standard. The samples were cooled to −50°C, kept for 15 min at this temperature, and then heated from −50°C to 250°C with a heating rate of $5°C\,min^{-1}$.

2.4. *SOD-mimic activity assay*

The SOD-mimic activity was determined by an indirect method adapted from Starha *et al.* [23]. This method is based on the competitive reaction of the tested compounds (**1–4**) and XTT dye [2,3-bis(2-methoxy-4-nitro-5-sulfophenyl)-2H-tetrazolium-5-carboxanilide sodium salt] with a saturated DMF solution of potassium superoxide (KO_2). The interaction of XTT dye with superoxide anion radical led to the formation of XTT–formazane, whose concentration was determined by spectroscopic measurements at 480 nm. The tested complexes, which acted as scavengers for superoxide anion radicals, decreased the absorbance at 480 nm. The SOD-mimic activity was expressed as the IC_{50} value, calculated from the concentration-dependent curve of the inhibition of the absorbance at 480 nm at eight concentration levels.

The required amounts of $1.00 \times 10^{-3}\,mol\,L^{-1}$ DMF solutions of the tested complexes were added to $1.0 \times 10^{-2}\,mol\,L^{-1}$ potassium phosphate buffer (pH 7.4) to provide 0.125, 0.250, 0.500, 0.750, 1.00, 2.50, 5.00, 7.50, and $10.0 \times 10^{-16}\,mol\,L^{-1}$ ($\mu mol\,L^{-1}$) solutions. Subsequently, 500 µL of XTT dissolved in buffer were added and the resulting solution was mixed thoroughly. The reaction was started by the addition of 500 µL of a saturated KO_2 solution in DMF. In all cases, the final volume was 3.00 mL and five samples of each concentration level of all the copper(II) complexes were tested ($n = 5$). After the incubation for 30 min at room temperature, the absorbance at 480 nm was measured against a blank sample prepared without the XTT dye. The same procedure was used to prepare the control sample without the tested copper(II) complexes and the absorbance was measured against a solution containing only XTT dye. The percentages of inhibition (% INH) were determined according to the formula $(1 - X\text{sample}/X\text{control}) \cdot 100 \pm (S^2\text{sample} + S^2\text{control})^{1/2} \cdot 100\%$, where X is the media of the absorbance values obtained and S the standard deviation of the absorbance. The IC_{50} values represent the concentrations of the tested copper(II) complexes reducing XTT–formazane formation to 50%.

2.5. *Evaluation of anti-inflammatory properties*

To evaluate the anti-inflammatory activity of **2**, carrageenan-induced paw edema assay was carried out as described by Winter *et al.* [24]. Female mice of about 30 g were randomly divided into three groups. Each group contained six mice fasted for 18 h. Test animals were administered orally an aqueous suspension of the copper(II) complex under study ($26\,mg\,kg^{-1}$) and the calcium salt of Fenoprofen ($22\,mg\,kg^{-1}$). Each quantity of drug administered is equivalent to $20\,mg\,kg^{-1}$ of Fenoprofen. The vehicle alone was used as excipient for the control group. The drugs were suspended in carboxymethylcellulose at 0.1% and Tween 80 at 0.05% (1 : 1, v/v) just before use. Drug and excipient were orally administered in 0.5 mL of the corresponding

suspension to each animal 1 h before inducing edema in the left hind paw by sub-plantar injection of 0.05 mL of a 2% suspension of carrageenan.

The length of the paw was measured with a digital electronic caliber "Caliper" (0.1 mm resolution) immediately before the injection of carrageenan and 3, 5, 7, and 9 h after the injection. The anti-inflammatory effect of the test was expressed in terms of the percent inhibition of edema produced by each drug-treated group and was calculated as $[(\Delta C - \Delta T)/\Delta C] \times 100$, being ΔC the mean of the control group and ΔT the mean of the test group. The data were expressed as mean ± standard error of media (S.E.M.).

To determine the significant differences between the mean response of each treated group and the control group, Student's *t*-test has been applied. It was also determined the difference in the mean response between the group treated with the complex and the one treated with Fenoprofen calcium salt. Statistical significance was set as $p < 0.05$.

3. Results and discussion

3.1. *Dinuclear tetracarboxylates*

The green complex **1** has a typical dinuclear paddle-wheel "$Cu_2(fen)_4$" molecular arrangement with two dmf molecules in the axial positions of the square pyramidal coordination spheres of copper [25]. When the axial positions are replaced by diazines, in 1 : 1 molar proportion, slightly soluble complexes are obtained. As reported for other copper(II) carboxylates, the dinuclear paddle-wheel subunits are connected by the diazines as bridges in uni-dimensional (1-D) polymeric structures (scheme 2) [21, 26].

The new substances **2–4** were insoluble in water and light alcohols, but soluble in DMF and DMSO with the breakage of the polymeric chains (section 3.5). The green solids had pseudo-microcrystalline appearance but behaved as glassy solids when studied by X-ray diffraction.

3.2. *EPR spectra*

EPR spectra of the microcrystalline complexes **2–4** at room temperature resemble those of many other tetracarboxylate-bridged dinuclear Cu(II) complexes (figure 1 and table 1), with well-known paddle wheel "$Cu(II)_2$–$(RCOO)_4$" cages, wherein the zero field splitting (D) is significantly greater than hv and E 0 (axial symmetry) [27, 28].

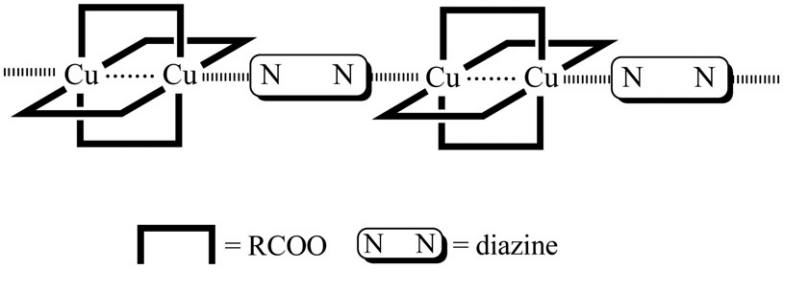

Scheme 2. Molecular arrangement in polymeric copper(II) carboxylates with diazines.

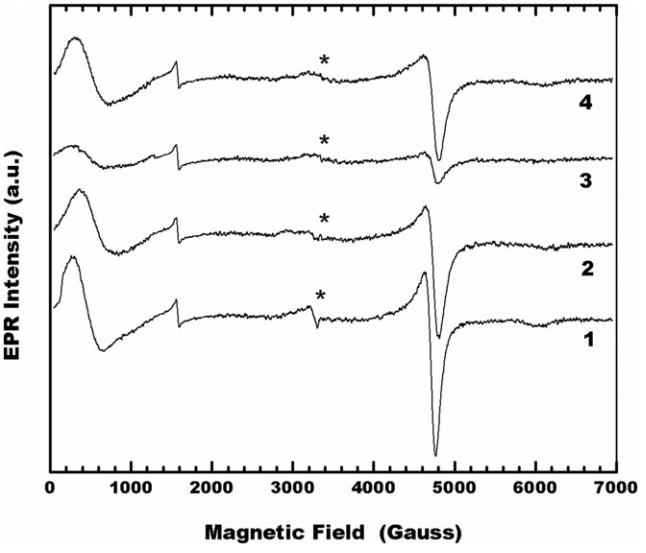

Figure 1. X-band EPR spectra of powdered dinuclear complexes $[Cu_2(fen)_4(dmf)_2]$ (**1**), $[Cu_2(fen)_4(4,4'\text{-bipy})_n$ (**2**), $[Cu_2(fen)_4(pyz)]_n$ (**3**), and $[Cu_2(fen)_4(2,5\text{-}Me_2pyz)]_n$ (**4**) at room temperature asterisk (*) denotes small signals due to monomeric impurities.

Table 1. X-band EPR data[a] of **1–4**.

Compounds	Hz1 (G)	H⊥ (G)	Hz2 (G)	$g\perp$	gz
$[Cu_2(fen)_4(dmf)_2]$ (**1**)[b]	502	4590	6080	2.14	2.49
$[Cu_2(fen)_4(4,4'\text{-bipy})]_n$ (**2**)	629	4740	6210	2.19	2.50
$[Cu_2(fen)_4(pyz)]_n$ (**3**)	532	4715	(6180)[c]	(2.19)[d]	(2.47)[d]
$[Cu_2(fen)_4(2,5\text{-}Me_2pyz)]_n$ (**4**)	557	4710	6080	2.20	2.52

[a]At room temperature.
[b]Reference [16].
[c]Very weak absorption.
[d]Only approximate values (section 3.2).

If the randomly oriented pair of Cu(II) ions have moderate interaction, the ground state of the dicopper is a singlet ($S=0$) and the triplet state ($S=1$) can be thermally populated. Thus, we expect to observe three absorptions around 600, 4700, and 6100 G corresponding to resonance fields Hz1, H⊥, and Hz2 of the six $\Delta M = \pm 1$ resonance fields [27]. The data obtained for **2**, **3**, and **4** (table 1) are in accord to earlier reports of similar Cu(II) dinuclear complexes [26, 27]. Small signals corresponding to mononuclear impurities (around 3200 G) are also observed. The quality of the spectra precludes a precise determination of the magnetic parameters. The g values reported in table 1 were calculated using the equipment frequency of 9.76 GHz and taking into account the simplified model for moderately interacting dinuclear Cu(II) centers [27, 28]. The calculated magnetic parameters obtained are in agreement to values reported for other dicopper(II)–tetracarboxylate complexes [22, 28–30]. Compound **3** with pyrazine shows weaker absorptions than the other complexes and the position of the Hz2 transition has little accuracy. The calculations used yield zero-field splitting parameters

(D) around 0.39 cm^{-1} for all the new substances, in accord with values reported for structurally related complexes. These results have been obtained taking into account the traditional calculations employed by many authors for this kind of complex. In a recent work negative values for D have been determined for dinuclear complexes [31].

3.3. *IR spectra*

Fenoprofen calcium salt, $Ca(fen)_2 \cdot 2H_2O$, has two characteristic bands at 1560 and 1420 cm^{-1} corresponding to asymmetric and symmetric stretching vibrations of carboxylate [18]. The IR spectra of the new copper(II) complexes reveal these bands shifted to 1626 and 1406 cm^{-1} for **2**, 1618 and 1408 cm^{-1} for **3**, and 1618 and 1408 cm^{-1} for **4**. These shifts indicate the coordination of fenoprofenate to copper(II). The measured shifts of those bands ($\Delta = 220$, 210, and 210 cm^{-1}) correspond to bridging coordination of the anions. A similar result was observed for $[Cu_2(fen)_4(dmf)_2]$ (**1**) [13] and for other dinuclear copper(II) carboxylate complexes with NSAIDs [32–34]. Selected FTIR bands of the complexes are shown in table 2. The assignments of fenoprofenate absorptions have been made taking into account vibrational studies on benzoic acid [35], dibromodiphenylether [36], ibuprofen [37, 38], and flurbiprofen [39].

The starting compound **1**, $Cu_2(fen)_4(dmf)_2$, has an absorption at 1668 cm^{-1} assignable to dmf coordinated to copper(II). This band is absent in IR spectra of the three compounds under study, indicating the replacement of dmf by the corresponding nitrogen ligand.

When analyzing absorption spectra of the 4,4′-bipyridine compound **2**, some bands assignable to the vibrations of the bridging diazine are clearly observed, shifted to higher wavenumbers (except the strong band at 759 cm^{-1}) when compared to the free base (1597vs, 1531 m, 1238 m, 1020 m, 831s, 614vs), indicative of coordination of 4,4′-bipy to metal [40, 41]. In particular, the band at 630 cm^{-1}, associated to a ring deformation of 4,4′-bipyridine, is very sensitive, indicative of bridging coordination to metal [42]. Another intense band of free bipyridine (1449s cm^{-1}) could not be assigned because it is obscured by strong absorptions of fenoprofenate.

A similar analysis for pyrazine and 2,5-Me_2pyz complexes, **3** and **4**, respectively, shows that the bands at 448 and 428 cm^{-1}, shifted respectively from 417 and 410 cm^{-1} in the free pyrazine ligands [43–46] are particularly diagnostic of bridging coordination. Bands at 769 and 751 cm^{-1}, respectively, for **3** and **4**, red-shifted from spectra of the free diazines (805 and 881 cm^{-1}) are also indicative of coordination to copper. Some other absorptions of the diazines shifted from the free ligands were also observed and assigned (table 2).

3.4. *Thermal analysis*

The thermal stabilities of **2–4** were analyzed between room temperature and 850°C with TGA and DTA methods, and between −50°C and 250°C with DSC.

For **3**, the pyrazine molecules are removed at 175°C but overlaps with the first endothermic complex degradation step of fenoprofenate, which occurs between 200°C and 350°C (Supplementary material). In this temperature range fenoprofenate could lose difenilether fragments as already proposed for **1** [13]. The successive events are evidenced by two endothermic peaks in the DTA curve, centered at 198°C and 213°C, that are

Table 2. IR data (KBr, 4000–400 cm^{-1}) of **1–4**.

1[a]	2	3	4	Assignments[b]
3063w[c]	3061w	3065w	3060w	ν(CH)
–	3022sh	3020sh	–	ν(CH) (L)[d]
2976sh	2964w	2968w	2978w	$\nu(CH_3)$
2927m	–	–	2931w	$\nu(CH_3)$ (dmf / L)
1668m	–	–	–	υ(CO) (dmf)
1612vs	1626vs	1618vs	1619vs	ν_{as}(COO)
–	1604vs	–	–	ν(CC), ν(CN) (L)
1580m	1580m	1582m	1582m	ν(CC)
–	1538w	–	–	ν(CC), ν(CN) (L)
1488m	–	–	–	$\delta_{as}(CH_3)$ (dmf)
–	–	–	1489m	ν(CC), ν(CN) (L)
1484s	1486s	1485s	1485s	ν(CC)
1441m	1442m	1441m	1445m	$\delta_{as}(CH_3)$
–	–	1414vw	–	ν(CC), δ(CH) (L)
1408s	1406s	1409s	1407s	ν_s(COO)
1385m	–	–	–	$\delta_{as}(CH_3)$ (dmf)
1371m	1367m	1368m	1366m	ν(CC)
–	–	–	1334m	$\delta_{as}(CH_3)$ (L)
–	1289m	–	–	δ(CH) (L)
1264s	1260s	1256m	1255sh	ν(CC)
1225s	1223s	1230s	1242s	ν_{as}(COC), δ(CCC)
1209w	1206w	1207m	1208m	ν_s(COC), δ(CCC)
1162m	1163m	1160m	1162m	δ(CH)
–	–	1132w	–	ν(CC), δ(CCC) (L)
1110m	–	–	–	ν(CN) (dmf)
–	1043w	1049m	–	ν(CC), δ(CCC) (L)
–	904m	–	–	δ(CH) (L)
881m,br	885m	884m	886m	$\rho(CH_3)$
–	810m	835w	813w	γ(CH) (L)
801m	788vw	788w	785w	γ(CH)
–	759s	769s	751m	γ(CH) (L)
733m	737m	729m	–	δ(COO)
695s	691s	694s	696s	γ(CH)
–	630m	–	640w	δ(CCC) (L)
487w	493w	485w	489w	γ(CCC)
452w	450w	454vw	459w	γ(CCC)
–	–	448m	428m	γ(CCC) (L)

[a]Reference [16].
[b]ν: stretching; δ: in-plane deformation; γ: out-of-plane deformation; ρ: rocking.
[c]v: very; s: strong; m: medium; w: weak.
[d]L: diazine.

confirmed by DSC analysis with two endothermic signals at 209°C ($\Delta H = 69\ J\ g^{-1}$) and 218°C ($\Delta H = 77\ J\ g^{-1}$) (figure 2). The total percent mass loss of 59.9% observed between 175°C and 350°C is in good agreement with the calculated loss of 61.5% (1 pyz + 4 diphenylether groups). The last degradation process is an exothermic mass loss step involving final decomposition of the anion residues (found: 27.4%; calculated: 24.9%). At 850°C CuO solid is obtained (found: 12.7%, calculated: 13.6%).

Due to the non-crystalline structure of the new substances, DSC analysis began from a low temperature (−50°C), looking for possible structural rearrangements (glassy transitions). As can be seen in figure 2, the polymeric complexes do not suffer structural changes at low temperatures.

For **2**, two degradation steps are observed (Supplementary material), showing a thermal decomposition process similar to **1** or **3**. In the first long, endothermic, and

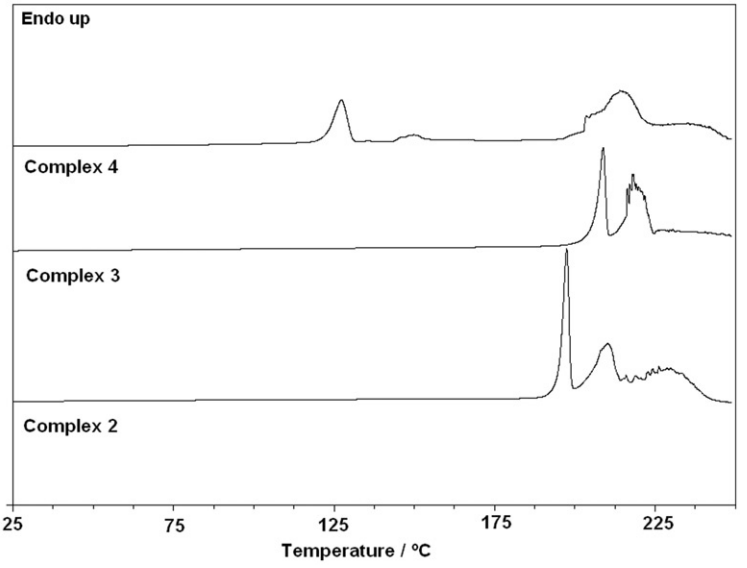

Figure 2. DSC analysis for powdered $[Cu_2(fen)_4(L)]_n$ complexes (L = 4,4′-bipy (**2**), pyz (**3**), and 2,5-Me_2pyz (**4**)) under N_2 flux ($20\,cm^3\,min^{-1}$). Heating rate: $5^\circ C\,min^{-1}$.

complex process between 160°C and 375°C, 4,4′-bipyridine degradation and partial decomposition of fenoprofenate occur simultaneously (total percent mass loss observed: 64.8%; calculated: 65.8%). The DTA curve shows three signals at 178°C, 194°C, and 213°C, as well as in the DSC curve at 197°C, 210°C, and *ca* 222°C with ΔH values of 88 and $62\,J\,g^{-1}$, respectively (figure 2). The degradation process finishes with a second exothermic mass loss involving decomposition of the anion residues (found: 21.1%; calculated: 20.2%). Finally, at 850°C solid CuO is obtained (percent mass of residue observed: 14.1%, calculated: 12.6%).

Complex **4**, containing 2,5-dimethylpyrazine ligands, shows a different degradation pattern than **1**, **2**, and **3** (Supplementary material). Between 125°C and *ca* 220°C incomplete volatilization of 2,5-dimethylpyrazine is produced (mass loss observed: 7.3%; calculated: 9.0%) (Supplementary material). This first degradation step is also evidenced by endothermic peaks at 129°C in DTA, 127°C and 150°C in DSC analysis, respectively (figure 2). The second step between 220°C and 320°C presents a greater mass loss than in the other complexes (observed: 75.1%), with an endothermic beginning (broad peak at 214°C in DSC curve) and exothermic ending. The strong difference between fragmentation of fenoprofenate in **4** against **2** and **3** is surprising. The identity of the fragments is unknown. The process finishes with complete degradation of fenoprofenate (mass loss observed: 5.2%) until residual solid CuO is obtained (observed: 13.8%; calculated: 14.6%).

3.5. *UV-Vis spectra*

Electronic spectra as Nujol mulls of the solid Fenoprofen–copper(II) complexes exhibit one broad asymmetric band in the visible region of the electromagnetic spectrum,

around 700 nm (Band I in table 3) and strong unresolved absorptions in the UV region (Supplementary material).

In DMF solutions a second absorption (Band II) is now easily observed at *ca* 380 nm, which is characteristic of the bridging Cu–OCO–Cu linkage in dinuclear copper complexes [31, 47]. Sometimes Band II has been erroneously assigned to another low absorption appearing around 320 nm for monomeric carboxylates [48] or arising from a transition of the triplet state of the dinuclear complexes [49]. The presence of Band II in the DMF spectra of **2–4** shows clearly that the dinuclear paddle-wheel unit of the solid complexes is still present in solution. For dicopper carboxylates soluble in light alcohols it has been reported that Band II disappears in solution with the decomposition of the paddle-wheel units [50]. The differences in the absorptivity values of the bands (Band I or Band II) between the four complexes would indicate that the nitrogen ligands remain coordinated to Cu(II) of the dinuclear units, as also reported by Abuhijleh [22] for $[Cu_2(val)_4(4,4'\text{-bipy})]_n$ (val = valproate anion). The expected aromatic $\pi \rightarrow \pi^*$ absorptions of the diazines and the fenoprofenates are masked by intense UV absorptions of DMF. For dinuclear copper tetracarboxylates a third very intense absorption assignable to a carboxylate−Cu(II) charge-transfer transition (Band III) [47] is expected around 260 nm, a spectral zone here dominated by DMF absorptions.

Bands I–III have been observed in UV-Vis spectra of many binuclear copper(II)–carboxylate complexes. From papers of Dubicki [51] and Tsuchida *et al.* [52], Band I has been assigned to the $d_{zx/yz} \rightarrow d_{x^2-y^2}$ transitions of tetragonally distorted Cu(II). The shoulder at the lower energy side of Band I was assigned to the $d_{z^2} \rightarrow d_{x^2-y^2}$ transitions of Cu(II) [47]. Bands II and III were recognized as ligand–metal charge-transfer transitions of the "$Cu_2(RCOO)_4$" framework [47, 53]. As far as we know, no systematic analysis of the dependence of the UV-Vis absorptions with the structure of the axial ligand for $[Cu_2(RCOO)_4(L)]$ or $[Cu_2(RCOO)_4(L)_2]$ complexes, when L is an azine or diazine molecule, has been reported. The wide range of bibliographic data has been obtained in very different experimental conditions [54]. The work of Kato and Muto [53] is about the influence of simple axial ligands as substituents on the carboxylate anions over the UV-Vis absorptions. Taking into account the conclusions of that report and the accepted model for UV-Vis absorptions in dicopper-tetracarboxylates, the blue shift of Band I (solid) and red shift of Band II (DMF) from **2** to **4** could be assigned to a weakening of the Cu(II)–L interaction. This conclusion must be considered taking into account the recent article of Kyuzou *et al.* [55]. From new experimental and theoretical data of $Cu_2(CH_3COO)_4{\cdot}2H_2O$, these authors propose a different origin for Band I. Their calculations indicate that not only copper(II) orbitals but carboxylate orbitals are also involved in the MO related to Band

Table 3. UV-Visible absorptions [nm/ϵ (L mol^{-1} cm^{-1})] for **1–4**.

	Band I[a]		Band II[a]
Compound	Nujol	DMF	DMF
$[Cu_2(fen)_4(dmf)_2]$ (**1**)	699	704/423	375/270
$[Cu_2(fen)_4(4,4'\text{-bipy})]_n$ (**2**)	700	705/491	380/245
$[Cu_2(fen)_4(pyz)]_n$ (**3**)	699	704/419	385/210
$[Cu_2(fen)_4(2,5\text{-}Me_2pyz)]_n$ (**4**)	692	704/382	390/170

[a]See section 3.5 for assignments.

I transitions (the main absorption and the low energy side band). The work of Kyuzou *et al*. [55] confirms the charge-transfer character of Band II and its origin in the singlet electronic state of a tetracarboxylate bridged weak antiferromagnetically interacting dicopper(II) moiety.

3.6. *SOD-mimic activity*

Cu,Zn–SOD is a metalloprotein which catalyzes the scavenging of superoxide O_2^-. Copper is present in the catalytic centre and undergoes reduction–oxidation cycling during the dismutation of O_2^-. Zinc ion is not involved in this cycle but facilitates the oxidation by maintaining the configuration of the active site [56]. Attention has been paid to the development of synthetic analogues of SOD. In this context it has been proved that many Cu–NSAIDs complexes exhibit SOD activity [1], so one of the aims of this work was to study the superoxide scavenging activity of the new complexes. SOD activity was observed in all the substances and showed a dependence with the type of ligand bonded to copper(II).

Figure 3 shows the results for the *in-vitro* SOD-mimic activity for **1–4**. This property has been evaluated comparing IC_{50} values of the compounds (figure 4). All the complexes studied, except **4**, present lower IC_{50} values than the native bovine

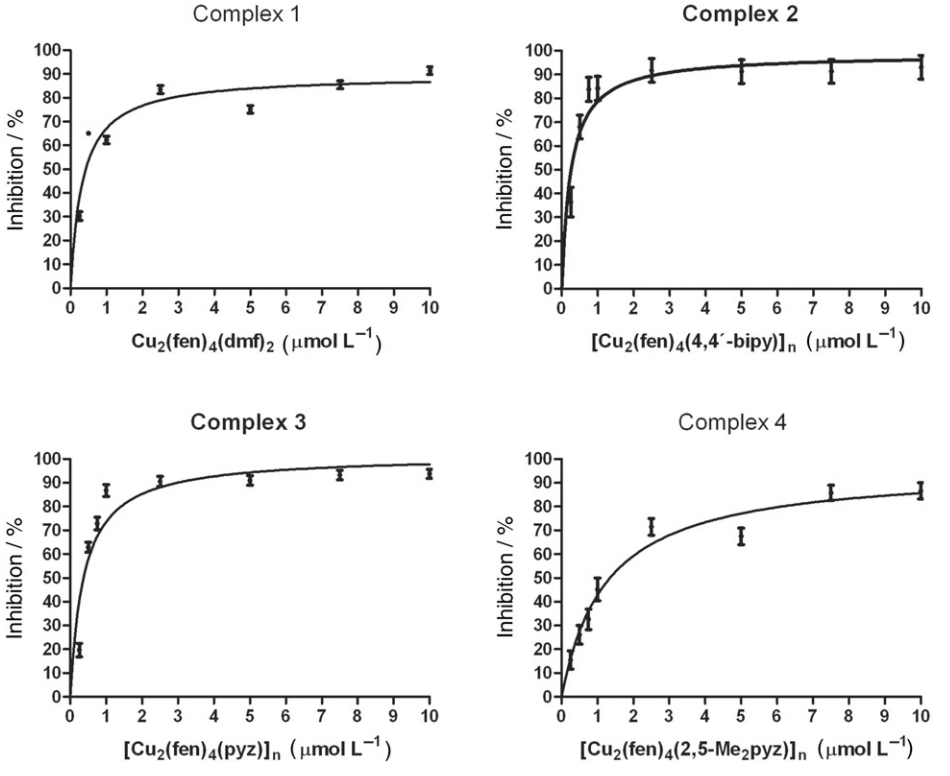

Figure 3. Percentage of inhibition of XTT reduction with an increase in concentration of the complexes. The curves have been obtained in DMF at 25°C.

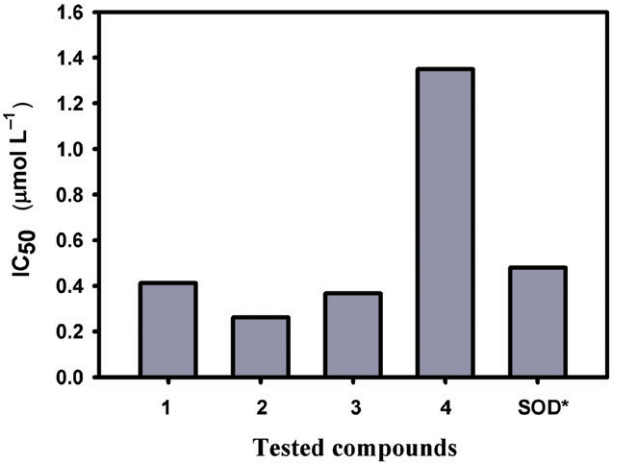

Figure 4. Results of *in-vitro* SOD-mimic activity testing for **1–4** with the native bovine Cu,Zn–SOD*, expressed as IC_{50} (*mol L^{-1}). *Extracted from reference [23].

Table 4. *In-vitro* SOD-mimic activity (IC_{50}) of Cu–NSAID complexes.

Copper complex	IC_{50} (μmol L^{-1})	Method[a]	Refs.
$[Cu(asp)_2(py)_2]$[b]	13	A	[55]
$[Cu_2(Indo)_4(dmf)_2]$[c]	2–25[d]	B	[55]
$[Cu_2(Indo)_4(dmf)_2]$	0.23	C	[55]
$[Cu_2(tolf)_4(dmf)_2]$[e]	1.97	C	[55]
$[Cu_2(Nap)_4]$[f]	0.30	C	[56]
$[Cu_2(val)_4]$[g]	10.4	D	[22]
$[Cu(val)_2(4,4'\text{-bipy})]_n$	18.3	D	[22]
$[Cu_2(val)_4(4,4'\text{-bipy})]_n$	5.0	D	[22]
$[Cu_2(\mu\text{-HL1})_4Cl_2]Cl_2{\cdot}2H_2O$[h]	1.090	E	[23]
$[Cu_2(\mu\text{-HL2})_4Cl_2]Cl_2{\cdot}2H_2O$[i]	0.687	E	[23]
$[Cu_2(fen)_4(dmf)_2]$ (**1**)	0.411	F	This work
$[Cu_2(fen)_4(4,4'\text{-bipy})]_n$ (**2**)	0.261	F	This work
$[Cu_2(fen)_4(pyz)]_n$ (**3**)	0.367	F	This work
$[Cu_2(fen)_4(2,5\text{-}Me_2pyz)]_n$ (**4**)	1.350	F	This work
Cu,Zn–SOD native bovine	0.480	E	[23]
Cu,Zn–SOD	0.04	B	[57]
Cu,Zn-SOD native	0.72	D	[22]

[a]A: NBT/alkaline dmso; B: NBT/pulse radiolysis/dmso; C: NBT/xanthine-xanthine oxidase/dmso; E: XTT/O_2^-/dmso; F: XTT/O_2^-/dmf.
[b]Asp: aspirinate.
[c]Indo: indomathacinate.
[d]Solvent dependent.
[e]Tolf: tolfenamate.
[f]Nap: naproxenate.
[g]Val: valproate.
[h]HL_1: 6-[(2-methoxybenzyl)amino]purine.
[i]HL_2: 6-[(4-methoxybenzyl)amino]purine.

Cu,Zn–SOD enzyme ($IC_{50} = 0.480\,\mu mol\,L^{-1}$) evaluated by Starha *et al.* [23]. Complex **1** has an IC_{50} of $0.411\,\mu mol\,L^{-1}$ while **2** and **3** have lower values (0.261 and $0.367\,\mu mol\,L^{-1}$, respectively); **4** has a higher value of $1.350\,\mu mol\,L^{-1}$. The SOD-mimic activity of **2** and **3** is comparable to the best SOD-mimic behaviors reported for Cu(II)–NSAID complexes (table 4).

Table 5. Anti-inflammatory activity in carrageenan-induced paw edema in mice.

	Δ mm (mean ± S.E.M)[a]			
Groups	3 h	5 h	7 h	9 h
Control	1.56 ± 0.08	1.71 ± 0.09	1.80 ± 0.09	1.67 ± 0.09
Fenoprofen salt	0.93 ± 0.12	0.89 ± 0.14	1.32 ± 0.09	1.31 ± 0.21
Complex **2**	1.02 ± 0.07	1.15 ± 0.08	1.33 ± 0.12	1.33 ± 0.14

[a]Mean values of the difference of the length of the hind paw with respect to the beginning of the assay.

In the native Cu,Zn–SOD the mechanism of scavenging involves replacement of a water molecule, located in the axial position, by O_2^-, in order to catalyze its dismutation. In the model proposed for the complexes under study their polymeric structure should be broken in DMF so the catalytic unit would present the structure $Cu_2(Fen)_4(dmf)(L)$. The mechanism proposed for these complexes consists in the replacement of dmf by the superoxide radical and a subsequent electron transfer to the dinuclear framework. The presence of the second copper(II) in the dinuclear units would cooperate in the electron transfer and contribute to the higher activity than the native bovine enzyme [23]. The presence of the nitrogen-donor ligand would regulate the SOD-mimic activity. In **2** and **3**, it appears that the presence of 4,4′-bipyridine or pyrazine coordinated to one side of the dinuclear framework has a beneficial effect over the electron transfer between the coordinated O_2^- and the dinuclear framework, compared to **1**. When the axial position is occupied by a weaker ligand as 2,5-Me_2pyz in **4** the SOD-mimic activity is lower.

3.7. *Anti-inflammatory properties*

One proposed mode of action of Cu–NSAID complexes is their SOD-mimic activity. The ability to scavenge O_2^- could be responsible for the more potent anti-inflammatory activity when compared to the uncomplexed parent drug [1]. The therapeutic properties of a substance also depend on its bioavailability and biodistribution. Thus, its solubility in biological fluids could be a determinant for its activity and responsible for the lack of correlation with other properties determined *in vitro*.

Taking into account that **2** has the highest SOD-mimic activity evaluated by the XTT method, we selected it to evaluate anti-inflammatory activity in mice paw carrageenan-induced edema, in comparison to the Fenoprofen calcium salt (uncomplexed parent drug). Table 5 shows the results obtained for this assay.

The study of acute anti-inflammatory test showed that **2** inhibited the inflammation during the assay with respect to the control, presenting no significant differences in comparison to Fenoprofen calcium. Figure 5 shows the inflammation inhibition percent; at the third and fifth hours of the experiment the inflammation inhibition percent was still lower than Fenoprofen calcium salt, equaling the percentage at the last time of the assay (seventh and ninth hours). Complex **1** exhibited a significant difference when compared to Fenoprofen calcium salt at the seventh hour of the experiment and maintained its performance until the end of the assay [13]. We did not observe this tendency for the complex under study. By this way, we did not find correlation between

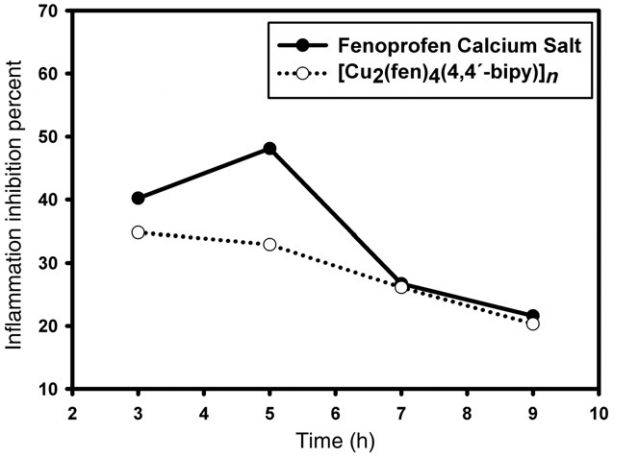

Figure 5. Inflammation-inhibition percent in carrageenan-induced paw edema in mice.

the SOD-mimic activity and the anti-inflammatory properties of **2**. The reason could be a lower solubility of **2** than **1** in biological fluids, interfering with bioavailability and biodistribution of the copper(II) complex affecting directly its therapeutic properties.

4. Conclusions

Three new dinuclear copper(II) complexes with Fenoprofen were synthesized and characterized. The results of the spectroscopy (EPR, IR, and UV-Visible) and thermal analysis, in comparison to $[Cu_2(fen)_4(dmf)_2]\cdot 2H_2O$ previously reported, shows general formula $[Cu_2(fen)_4(L)]_n$, where L are 4,4′-bipyridine, pyrazine, and 2,5-dimethylpyrazine.

SOD-mimic activity evaluated by the XTT method showed that three of the four complexes have higher activity than the native Cu,Zn–SOD; the 4,4′-bipyridine complex was most active ($IC_{50} = 0.260\,\mu mol\,L^{-1}$) followed by pyrazine compound, with an IC_{50} of $0.367\,\mu mol\,L^{-1}$ and finally 1, with an IC_{50} value of $0.411\,\mu mol\,L^{-1}$. The 2,5-dimethylpyrazine complex presented the lowest SOD-mimic activity. The SOD-mimic activity of the new complexes is comparable to the best SOD-mimic behaviors reported for Cu(II)–NSAID complexes; they present excellent anti-oxidant properties.

Anti-inflammatory properties of $[Cu_2(fen)_4(4,4'\text{-bipy})]_n$ evaluated by carrageenan-induced paw edema in mice showed no significant differences in its activity when compared to the uncomplexed parent drug calcium fenoprofenate. This result permits us to conclude that not all copper(II) complexes with AINEs have enhanced anti-inflammatory activity when compared to the free drug. There are many factors which could influence activities, such as solubility, chemical structure, and intrinsic characteristics of the complexes that modify their biodistribution and bioavailability.

Acknowledgments

M.A. Agotegaray and O.V. Quinzani thank SGCyT-UNS for financial support (Project 24/Q025). The authors would like to thank Dr Carlos Brondino (Departamento de Física, FBCB-UNL, Santa Fe, Argentina) for kindly registering the EPR spectra of the copper complexes and to Lic. Cecilia Ballesteros and Dra. Mariana Alvarez (INQUISUR, Universidad Nacional del Sur, Bahía Blanca, Argentina) for the determination of copper by Atomic Absorption spectroscopy. M.A. Agotegaray is fellow of CONICET (Consejo Nacional de Investigaciones Científicas y Técnicas).

References

[1] J.E. Weder, C.T. Dillon, T.W. Hambley, B.J. Kennedy, P.A. Lay, J.R. Biffin, H.L. Regtop, N.M. Davies. *Coord. Chem. Rev.*, **232**, 95 (2002).
[2] J.R.J. Sorenson. In *Handbook of Metal–Ligand Interaction in Biological Fluids: Bioinorganic Medicine*, G. Berthon (Ed.), Vol. 2, Marcel Dekker, New York (1995).
[3] L.-O. Klotz, U. Weser. In *Copper and Zinc in Inflammatory and Degenerative Diseases*, K.D. Rainsford, R. Milanino, R.J.R. Sorenson, G.P. Velo (Eds), Kluwer Academic Publications, Dordrecht (1998).
[4] D.H. Brown, W.E. Smith, J.W. Teape. *J. Med. Chem.*, **23**, 729 (1980).
[5] J.R.J. Sorenson. *Prog. Med. Chem.*, **26**, 437 (1989).
[6] V. Albergoni. In *Copper and Zinc in Inflammatory and Degenerative Diseases*, K.D. Rainsford, R. Milanino, J.R.J. Sorenson, G.P. Velo (Eds), Kluwer Academic Publications, Dordrecht (1998).
[7] E.J. Baran, C.C. Wagner, M.H. Torre. *J. Braz. Chem. Soc.*, **13**, 576 (2002).
[8] J.R.J. Sorenson. *Chem. Brit.*, **20**, 1110 (1984).
[9] R. Milanino, M. Marrella, G.P. Velo, P. Cristofori, A. Terron. In *Copper and Zinc in Inflammatory and Degenerative Diseases*, K.D. Rainsford, R. Milanino, J.R.J. Sorenson, G.P. Velo (Eds), Kluwer Academic Publications, Dordrecht (1998).
[10] R. Nickander, W. Marshall, J.L. Emmerson, G.C. Todd, R. McMahon, H.W. Culp. In *Pharmacological and Biochemical Properties of Drug Substances*, M.E. Goldberg (Ed.), American Pharmacological Association, Washington (1977).
[11] R.N. Brogden, R.M. Pinder, T.M. Speight, G.S. Avery. *Drugs*, **13**, 241 (1977).
[12] R.A. Appleton, K. Brown. *Prostaglandins*, **28**, 29 (1979).
[13] M.A. Agotegaray, M.A. Boeris, O.V. Quinzani. *J. Braz. Chem. Soc.*, **21**, 2294 (2010).
[14] S. Oga, S.F. Taniguchi, R. Najjar, A.R. Souza. *J. Inorg. Biochem.*, **41**, 45 (1991).
[15] A. Neves, L.M. Rossi, A.J. Bortoluzzi, A.S. Mangrich, W. Haase, R. Werner. *J. Braz. Chem. Soc.*, **12**, 747 (2001).
[16] J.M. McCord, I. Fridovich. *J. Biol. Chem.*, **244**, 6049 (1969).
[17] M. Valko, D. Leibfritz, J. Moncol, M.T. Cronin, M. Mazur, J. Teleser. *Int. J. Biochem. Cell Biol.*, **39**, 44 (2007).
[18] G. Rotilio, M.R. Ciriolo, M.T. Carri, L. Rossi. In *Handbook of Copper Pharmacology and Toxicology*, E.J. Massaro (Ed.), Humana Press, Totowa (2002).
[19] B.Q. Ma, S. Gao, J. Yi, G.X. Xu. *Polyhedron*, **20**, 1255 (2001).
[20] A. Corma, H. García, F.X. Llabrés i Ximena. *Chem. Rev.*, **110**, 4606 (2010).
[21] D.J. Tranchemontagne, J.L. Mendoza-Cortés, M. O'Keeffe, O.M. Yaghi. *Chem. Soc. Rev.*, **38**, 1257 (2009).
[22] A.L. Abuhijleh. *J. Inorg. Biochem.*, **68**, 167 (1997).
[23] P. Starha, Z. Travnicek, R. Herchel, I. Popa, P. Suchy, J. Vanco. *J. Inorg. Biochem.*, **103**, 432 (2009).
[24] C.A. Winter, E.A. Risley, G. Nuss. *Proc. Soc. Exp. Bio. Med.*, **111**, 544 (1962).
[25] M.A. Agotegaray, O.V. Quinzani, R. Faccio, C. Goyenola, A. Mombrú. *Acta Crystallogr. E*, **64**, 1612 (2008).
[26] J. Boonmak, S. Youngme, N. Chaichit, G.A. van Albada, J. Reedijk. *Cryst. Growth Des.*, **9**, 3318 (2009).
[27] P. Mosae Selvakumar, E. Suresh, P.S. Subramanian. *Inorg. Chim. Acta*, **361**, 1503 (2008).
[28] C.J. Williams, H. Morris, J. Svorec, M. Valkova, M. Valko, J. Moncol, M. Manzur, F. Valach, M. Melnik. *J. Mol. Struct.*, **659**, 53 (2003).
[29] Y. Muto, M. Nakashima, T. Tokii, I. Suzuki, S. Ohba, O.W. Steward, M. Kato. *Bull. Chem. Soc. Jpn.*, **75**, 511 (2002).
[30] J.L. Meier, C.E. Coughenor, J.A. Carlisle, G.O. Carlisle. *Inorg. Chim. Acta*, **106**, 159 (1985).

[31] M. Perec, R. Baggio, R.P. Sartoris, R.C. Santana, O. Peña, R. Calvo. *Inorg. Chem.*, **49**, 695 (2010).
[32] A.L. Abuhijleh. *J. Inorg. Biochem.*, **55**, 255 (1994).
[33] B. Viossat, F.T. Greenaway, G. Morgant, J.C. Daran, N.-H. Dung, J.R.J. Sorenson. *J. Inorg. Biochem.*, **99**, 355 (2005).
[34] Y.R. Morgan, P. Turner, B.J. Kennedy, T.W. Hambley, P.A. Lay, J.R. Biffin, H.L. Regtop, B. Warwick. *Inorg. Chim. Acta*, **324**, 150 (2001).
[35] M. Pagannone, B. Fornari, G. Mattei. *Spectrochim. Acta A*, **43**, 621 (1987).
[36] S. Qiu, X. Tan, K. Wu, A. Zhang, S. Han, L. Wang. *Spectrochim. Acta A*, **76**, 429 (2010).
[37] M. Smith, K. Stambaugh, L. Smith, H.-J. Son, A. Gardner, S. Cordova, K. Posey, D. Perry, A.S. Biris. *Vibrat. Spectrosc.*, **49**, 288 (2009).
[38] A. Jubert, M.L. Legarto, N.E. Massa, L. López-Tévez, N.B. Okulik. *J. Mol. Struct.*, **783**, 34 (2006).
[39] S. Sagdinc, H. Pir. *Spectrochim. Acta A*, **73**, 181 (2009).
[40] Z. Zhuang, J. Cheng, X. Wang, B. Zhao, X. Han, Y. Luo. *Spectrochim. Acta A*, **67**, 509 (2007).
[41] A. Topacli, S. Akuyz. *Spectrochim. Acta A*, **51**, 633 (1995).
[42] J.G. Contreras, C.J. Diz. *J. Coord. Chem.*, **16**, 245 (1987).
[43] F. Billes, H. Mikosh, S. Holly. *J. Mol. Struct. (Theochem)*, **423**, 225 (1998).
[44] T. Otieno, S.J. Rettig, R.C. Thompson, J. Trotter. *Can. J. Chem.*, **67**, 1964 (1989).
[45] J.F. Arenas, S.P. Centeno, J. López-Tocón, J.C. Otero. *J. Mol. Struct.*, **744–747**, 289 (2005).
[46] H. Endrédi, G. Billes, G. Keresztury. *J. Mol. Struct. (Theochem)*, **677**, 211 (2004).
[47] A.B.P. Lever. *Inorganic Electronic Spectroscopy*, 2nd Edn, Elsevier, New York (1984).
[48] M. Melnik, I. Potocnak, L. Macaskova, D. Miklos, C.E. Holloway. *Polyhedron*, **15**, 2159 (1996).
[49] N. Kumar, A.K. Suri. *Proc. Indian Natl. Sci. Acad. A*, **46**, 565 (1980).
[50] P. Kögerler, P.A.M. Williams, B.S. Parajón-Costa, E.J. Baran, L. Lezama, T. Rojo, A. Müller. *Inorg. Chim. Acta*, **268**, 239 (1998).
[51] L. Dubicki. *Aust. J. Chem.*, **25**, 1141 (1972).
[52] R. Tsuchida, H. Nakamura, S. Yamada. *Nature*, **178**, 1192 (1956).
[53] M. Kato, Y. Muto. *Coord. Chem. Rev.*, **92**, 45 (1988).
[54] J.E. Weder, T.W. Hambley, B.J. Kennedy, P.A. Lay, D. MacLachlan, R. Bramley, C.D. Delfs, K.S. Murray, B. Moubaraki, B. Warwick, J.R. Biffin, H.L. Regtop. *Inorg. Chem.*, **38**, 1736 (1999).
[55] M. Kyuzou, W. Mori, J. Tanaka. *Inorg. Chim. Acta*, **363**, 930 (2010).
[56] A.M. Ramadan, M.M. EI-Naggar. *J. Inorg. Biochem.*, **63**, 143 (1996).
[57] R.G. Bhirud, T.S. Srivastava. *Inorg. Chim. Acta*, **173**, 121 (1980).